



HAL
open science

Experimental assessment of freezing-thawing resistance of rammed earth buildings

Lassana Bakary Traoré, Claudiane Ouellet-Plamondon, Antonin Fabbri,
Fionn Mcgregor, Fabrice Rojat

► **To cite this version:**

Lassana Bakary Traoré, Claudiane Ouellet-Plamondon, Antonin Fabbri, Fionn Mcgregor, Fabrice Rojat. Experimental assessment of freezing-thawing resistance of rammed earth buildings. *Construction and Building Materials*, 2021, 274, pp.121917 -. 10.1016/j.conbuildmat.2020.121917 . hal-03492637

HAL Id: hal-03492637

<https://hal.science/hal-03492637>

Submitted on 2 Jan 2023

HAL is a multi-disciplinary open access archive for the deposit and dissemination of scientific research documents, whether they are published or not. The documents may come from teaching and research institutions in France or abroad, or from public or private research centers.

L'archive ouverte pluridisciplinaire **HAL**, est destinée au dépôt et à la diffusion de documents scientifiques de niveau recherche, publiés ou non, émanant des établissements d'enseignement et de recherche français ou étrangers, des laboratoires publics ou privés.



Distributed under a Creative Commons Attribution - NonCommercial 4.0 International License

Experimental assessment of freezing-thawing resistance of rammed earth buildings.

Lassana Bakary Traoré^{a,b}, Claudiane Ouellet-Plamondon^c, Antonin Fabbri^a, Fionn McGregor^a, Fabrice Rojat^b

^a LTDS, UMR 5513 CNRS, ENTPE, Université de Lyon, 69100 Vaulx-en-Velin, France

^b CEREMA/DTerCE/DLL/RRMS/Géomatériaux, 69674 Bron, France

^c Ecole de Technologie Supérieure, Montréal, Canada

Abstract

The use of earth as a building material is worldwide encouraged thanks to its low environmental impact and its high hygrothermal performances. In wet and cold regions, the durability of earthen constructions is a major preoccupation because of water attack and frost damage. The variety of raw earth, compaction method and exposition to water increases the complexity to agree on a representative testing protocol to assess the frost resistance of earthen buildings. In this context, various molding and testing configurations are proposed to evaluate the impact of repeated freezing and thawing (F-T) cycles on earthen compacted samples. The experimental protocol is adapted from ASTM D560 standard which recommends 12 F-T cycles of $-23^{\circ}\text{C}/+23^{\circ}\text{C}$. A series of cylindrical samples were made from two types of earths (unstabilized and cement-stabilized) compacted following two compaction methods (dynamically and statically). They were experimentally investigated under two kinds of freezing-thawing cycles that can affect earthen buildings. One with water absorption aimed at reproducing the combined effect of capillary rise and frost action. The other one consisted in testing samples at their manufacture saturation ratio in a moist environment in order to analyze the frost resistance at early age. After each cycle, frost damage was evaluated through the amount of mass lost by scaling, as well as water content and the volume changes. The results indicated that surface scaling affected all samples exposed to freezing and thawing, even if cement stabilization upgraded frost resistance. The impact of the freeze-thaw cycles on water uptake within the samples was analyzed, and some considerations were given in order to develop a dedicated test to assess freezing-thawing resistance of earthen building materials in milder conditions.

Keywords: Earthen constructions, freezing-thawing, surface scaling, stabilized earth, durability.

Introduction

Nowadays, earthen materials represent a clear interest for sustainable constructions thanks to their low embodied energy and the great thermal inertia of earthen walls [1][2]. Raw earth is also a good hygroscopic material, it participates in the regulation of indoor moisture levels through its moisture buffering capacity [3]. Stable indoor humidity levels are recognized to improve indoor comfort and reduce the risk of mold growth. On the other side, due to its hydromechanical behavior, raw earth material suffers from limited mechanical performances under high humidity conditions. In particular, a drop in mechanical strength is observed when the material is subjected to a moist attack [4] [5]. For example, Bui et al. underlined that an increase of the water content from 2% to 12% leads to divide the compressive strength and the stiffness of soils of variable compositions compacted according to the Proctor procedure (energy of compaction equal to $0.6 \text{ kJ}/\text{dm}^3$) by, at least 4. [5].

Such abnormal increase of water content, which may lead to the collapse of earthen walls, may come from capillary rise at the wall base or by roof leakage. Rainfall or water splashing may increase water content locally at the wall surface, which could potentially create erosion, if the architectural design of the building and of its surroundings are not appropriate. Actually, in major cases, abnormal water uptake in earthen walls is due to some technical mistakes such as raising the ground level above the foundation wall or covering earthen walls with an impermeable coating. An impermeable coating can disturb the natural equilibrium of the wall water content which is strongly linked to the evaporation process at the wall surfaces (**Fig. 1**).

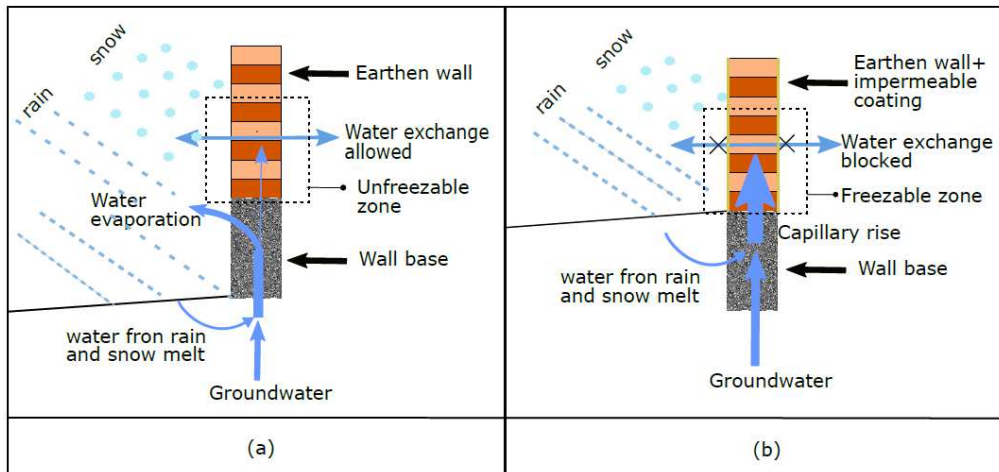


Fig. 1. (a) Earthen wall properly functioning with protection against capillary rise, (b) Risk of abnormal water content due to lack of protection against capillary rise

Additionally, the durability of earthen constructions is more jeopardized when moistening is associated with freezing and thawing. This combined action can expose buildings and structures to additional water uptake and cause severe damage. For example, Scarato et al. [6] reported that major collapses of earthen constructions in the Auvergne-Rhone-Alpes region in France had been recorded after thawing periods. They also underlined that earthen constructions are avoided during the winter period because of the great risk of frost damage at early age. The early age corresponds to the drying phase. After construction, the earthen wall manufactured at an initial saturation ratio close to 0.8 equilibrates with its environment and reaches saturation ratio levels below 0.2. During this early age that can last many months, the earthen material, which remains at relatively high saturation ratios may be far more vulnerable to frost damage if exposed to freezing temperatures.

In the general framework of common building materials like concrete and rocks, most of the physicochemical mechanisms leading to frost damage are nowadays well known. Two main types of deterioration mechanisms induced by repeated freezing and thawing cycles are generally considered: internal frost and surface scaling [7]. This latter is linked to a local flaking or peeling off the wall surface generally accelerated by the presence of deicing salts which induces a thermo-mechanical interaction between the frozen layer and concrete surface [8]. Also, Fabbri et al. [9] proved that frost scaling can occur without deicing salts because of the overpressure generated by ice crystallization at the frozen surface. The authors concluded that a high amount of ice and low permeability were key parameters to promote surface scaling. Internal frost damage is generally attributed to the volumetric increase of water during its solidification combined with the capillary transport of free water towards the freezing front. These two combined actions can generate an important hydraulic pressure [10][11] and significant water uptake [12], which can result in the modification of the porous network geometry [13][14] and damage the material [15][16][17]. With increasing numbers of freeze-thaw cycles, they both progressively induce many material properties modifications such as a loss in the mechanical strength and elastic modulus, an increase in intrinsic permeability and a volume change [14][18][19][21]. In addition, in frost-susceptible soils, the presence of micro-cracks and the cryopump action of the frozen zone on the unfrozen water can favor the development of ice lenses [21][22].

Since it influences both hydraulic pressures and water flow through the porous network, the initial liquid water saturation ratio appears to be one of the key factors driving the risk of damage by frost action [18]. Indeed, below a threshold value of saturation ratio, which depends on the material, but also on external parameters like amplitude and kinetic of the freezing-thawing cycles, no damage will occur [23]. For example, Aubert and Gasc-Barbier [24] have conducted freezing-thawing tests on unstabilized blocks and samples initially conditioned at 95%RH, which commonly leads to a saturation ratio between 0.1 and 0.3 for

earthen materials. Their results concluded that under such conditions freezing-thawing cycles do not damage the samples, but they lead to a progressive drying and hardening.

Some experimental methods have already been proposed to assess the freeze-thaw performances of earthen building materials. Generally, freezing-thawing cycles are carried out between -20°C to $+20^{\circ}\text{C}$ [25] but there is no consensus on their kinetic (from 4h to 24 h) and on thawing methods (in water or in open air) [26]. Most of the time, frost resistance of earth bricks was experimentally determined using direct methods based on visual inspection and mass loss after brushing. The threshold value of 25 freezing-thawing cycles without damage was proposed to identify frost-resistant earthen samples [27]. However, even if quite precise recommendations on brushing protocol have been edited, the variability of this direct method led several authors to replace it and/or to complete it with indirect methods such as the failure in mechanical strength, the change in pore structure or the rate of water absorption [28], [29], [26].

Even if these studies give first insights, there is yet no clear consensus on the experimental protocol that should be used to assess freeze-thaw resistance of earthen construction. In particular when they are in the classical field conditions of frost damage occurrence, that are at early ages (i.e. just after the fabrication and before the end of the drying stage of the wall) and/or when walls have to face with an abnormal increase of water content [6]. In addition, further parameters such as the stabilization or the compaction method are poorly investigated in the scientific literature.

In fact, among other techniques, earthen walls can be built by dynamic compaction in the case of rammed earth or by static compaction for compressed earth blocks. In the laboratory, dynamic compaction is obtained by using a universal Proctor machine and static compaction is set up by a strain-controlled or stress-controlled press. At the same water content and dry density, Seed et al. [30] observed that static-compacted soil samples exhibited higher mechanical strength than the ones which were dynamic-compacted whereas Ekwue et al. [31] demonstrated that the compaction method does not affect strength of samples compacted at the same moisture contents to same bulk densities. In general, compaction has a great impact on the mechanical behavior of soil specimens, optimal compaction improves the compressive strength. However, the comparison between static and dynamic compactions did not give clear conclusion on their mechanical impacts. Regarding the morphology of clayey matrix, Olivier [32] reported that the static compaction tended to produce a flocculated morphology whereas dynamic compaction led to a more disperse structure. These observations on the effects of the compaction method on microstructure may lead to differences in fluid transport through the porous network of press-compacted and dynamic-compacted raw earth samples.

In order to improve the mechanical strength and the water resistance of earthen materials, another solution consists in stabilizing the soil by adding between 5% to 12% of its dry mass, a binder like lime or cement [33]. For example, Kariyawasam and Jayansinghe [34] reported that water absorption and erosion rates are strongly minimized in cement-stabilized earthen materials. Also, an addition of 10% of cement allows multiplying the compressive strength by 2 or 3. Then it is shown that the higher the cement content, the better the mechanical performance [35]. Yet, it remains environmentally costly because 10% of cement in rammed earth, for example, represent large amounts of cement for a relatively low compressive strength when compared to other conventional materials [33]. Also, it is pointed out that cement stabilization reduces hygroscopic performances of raw earth materials [29, 30].

A large variation of degrees of saturation and manufacturing methods of earthen materials lead to some difficulties to find the key parameters of frost resistance and to predict its behavior when exposed to freeze-thaw cycles. In this context, this paper aims at studying the frost behavior at high saturation ratios of stabilized and unstabilized earthen materials, compacted by dynamic and static methods.

Let us underline that no dedicated test protocol exists for the evaluation of the performances of earthen building materials subjected to freeze-thaw cycles. In view of this lack, it was decided, in this study, to adapt the ASTM D560 [38] test method for freezing and thawing of compacted soil-cement mixtures.

2. Materials and methods

2.1. Materials

The soil used in this experimental study is extracted from Saint-Antoine l'Abbaye (STA), a village in a southeastern region of France called Auvergne-Rhône-Alpes. The full characterization of this soil has already been presented in [39]. As shown in **Fig. 2**, the original soil contained 16% of clay, 10% of silt, 29% of sand and 45% of gravels. Its plastic index is about 20% and its methylene blue value (MBV) is equal to 0.5, indicating the presence of poorly active clays. According to [1], this is a typical soil suitable for rammed earth construction. Before sample fabrication, the soil was sieved at 5 mm in order to keep a ratio higher than 10 between samples and larger grain sizes. Then the final composition of the soil used for the test was 28% of clay, 24% of silt, 38% of sand and 10% of gravels. Its grain size distribution is reported in **Fig. 2**

The cement used for stabilization is a Portland cement CEM II/32.5R. This type of cement with a content of 77% of clinker and 22% of limestone is commonly used to provide better mechanical behavior and water resistance of soils. The soil-cement formulation for stabilized earth is 10% cement per dry mass of soil. This mixture proportion was chosen in order to be compatible with standards of stabilized earth constructions that typically recommended an addition of 5% to 12% of cement [40].

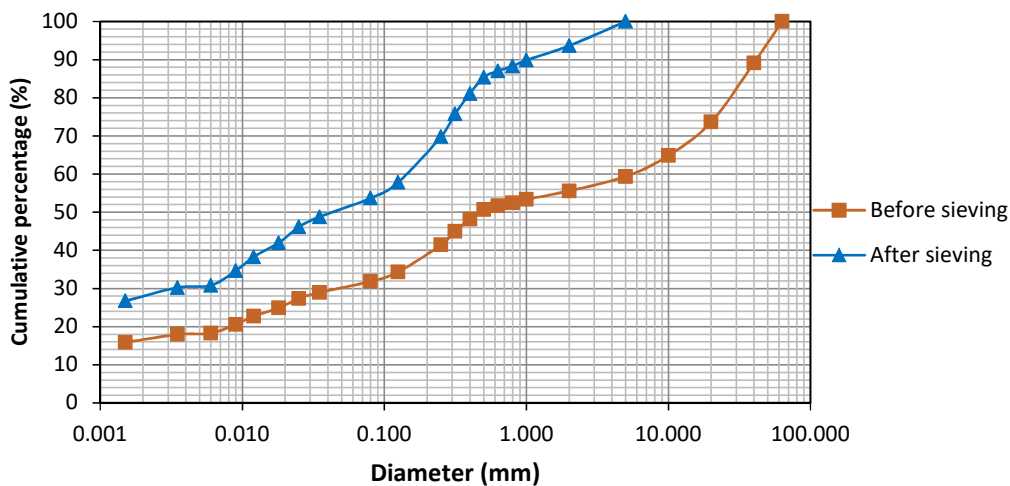


Fig. 2. The grain size distribution of the tested soil

2.2. Specimen preparation

The unstabilized and stabilized samples were both compacted at the Optimum Proctor characteristics (optimum water content and optimum dry density) determined in accordance with ASTM D558 [41]. It leads to 18% of optimum water content and 1.73 g/cm³ of optimum dry density for unstabilized soil, and to 17% of optimum water content and 1.72 g/cm³ of optimum dry density for stabilized soil. For each type of soil (stabilized and unstabilized), twelve samples were manufactured by using two different modes of compaction. A dynamic compaction in three layers was possible with an automatic Proctor machine following the manufacturing protocol detailed in [41]. A static compaction in two layers of 50.0 mm each was realized by using a mechanical press, which allowed a strain-controlled compaction at a speed of 1.25 mm/min. The compaction was controlled in displacement in order to obtain the same dry density than dynamic compacted samples. It led to a compaction axial stress of approximately 3 MPa per layer. It is worth to mention here that static compacted samples were not intended to reproduce the behavior of compacted earth blocks (CEB). Their aim was to test the effect of compaction procedures while all other parameters such as dry density, water content, and sample size were kept constant. That is why these samples were made with two layers and not in a single layer as for CEB.

After compaction, all the stabilized specimens were put in a moist room (RH=99+/- 0.5% and T=22+/-1°C) for a curing period of seven days conforming to ASTM D560. The unstabilized specimens were sealed in hermetic plastic bags to avoid moisture evaporation and stored in the controlled chamber during the curing period of stabilized samples. At the end of the seven-day storage, the diameter, the height and the water content of each sample were recorded as the reference state of samples before freezing and thawing. In conclusion, four types of samples are studied. The notations PRESS will be used to denote the samples compacted with a press (static compaction), while PROC will indicate the use of the Proctor device (dynamic compaction). The sample realized with unstabilized soil will be referenced as the US, while CEM will be used to specify the cement-stabilized soil. For each sample type, the skeleton density (ρ_s) was determined with a nitrogen pycnometer, and with the dry density (ρ_d), the porosity (ϕ) was estimated using the relation:

$$\phi = 1 - \frac{\rho_d}{\rho_s} \quad (1)$$

For each type (PRESS-US, PROC-US, PRESS-CEM and PROC-CEM), three supplementary samples were manufactured and used to conduct water absorption test following the experimental protocol described in [42]. An illustration of this experimental setup is presented in **Fig. 3**. The goal of this test is to determine the kinetics of capillary diffusion by considering the water absorption coefficient (A-value). This coefficient is related to the amount of absorbed water (kg) per unit of exposed surface (m²) and per square root of the duration of immersion (s^{1/2}).

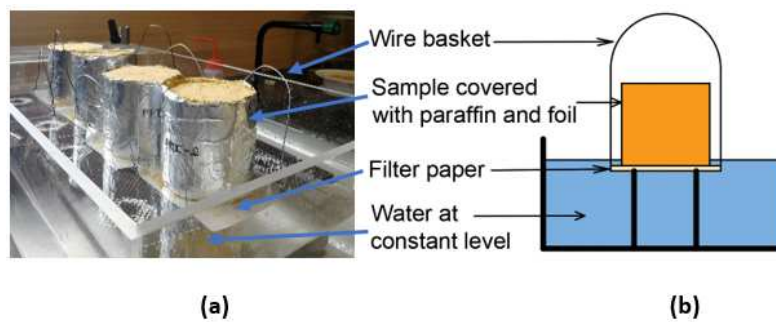


Fig. 3. Illustration (a) and schematic presentation (b) of the setup for water absorption test

The results of density measurements and absorption tests are presented in **Table 1**. The first remark that can be done is that the standard deviation calculated from the 3 water absorption tests of each sample type remains very small, especially for PRESS compacted samples. It is not a formal proof, but this result underlines the good repeatability in the sample fabrication, and it gives some confidence on the tendencies observed in the freezing-thawing experiments, even if only one sample was realized for each test configuration.

Concerning the obtained values, static compaction seems to provide significantly lower water absorption coefficient for both stabilized and unstabilized soils, while total porosity and soil nature are the same. This difference in A-Value confirms the strong impact of the compaction method on the porous network geometry. It tends to the conclusion that PRESS samples are less permeable to water and, thus, have a finer porosity than PROC ones. In addition, a higher heterogeneity may be expected for Proctor samples, which can lead to preferential migration pathways for the rising capillary water.

Going into details, a slightly lower water absorption can be observed for stabilized samples. This can be attributed to the presence of hydration products which limited the capillary continuity and protected the surface [21] [43].

Table 1. Main physical characteristics of each type of sample

Type	ρ_d (g/cm ³)	ρ_s (g/cm ³)	ϕ (%)	A-value (kg/m ² /s ^{1/2})	Standard deviation of A
PRESS-US	1.73	2.73	37	0.092	0.001
PROC-US				0.141	0.008
PRESS-CEM	1.72	2.71	36	0.075	0.001
PROC-CEM				0.124	0.009

2.3. Testing methods

Several methods have already been used to assess the freezing-thawing resistance of earthen materials. The three more used are reported in Table 2.

Table 2. Differences in experimental protocols for evaluating freeze-thaw durability

Protocol standard	ASTM D560	PN-EN 206	Iowa Freeze-Thaw
Preparations of samples	7 days at T=23°C and RH=100%	28 days at T=18°C and RH>90% Saturation with water	7 days of curing at T=25°C and RH>95% Immersion in distilled water for 1 day
Freezing conditions	-23°C for 24h	-18°C for 4h	-6.7°C (20F) at the top and 1.7°C at the bottom for 16h
Thawing conditions	+23°C for 23h	18°C for 2-4h	25°C (77F) for 8h
Moistening conditions	Defrosting with capillary absorption in moist room	Defrosting in water	
Measurements	Mass loss by brushing Change in water content volume changes	Loss of weight Decrease in compressive strength	Change in compressive strength Frost heave Change in moisture and distribution through the height of specimen

Both PN-EN 206 [26] and Iowa Freeze-Thaw [44] tests were not adapted to our studies since they require to immerse the sample in water, which is not possible for unstabilized earth. Then, we opted to ASTM D560 which provided a realistic F-T scenario in which water absorption is made by high relative humidity and capillary action. Let us underline that this experimental procedure was largely used to assess frost resistance of Compressed Earth Blocks [45] and for stabilized soils [46]. It is, however, important to keep in mind that some parameters of ASTM D560 method were largely criticized. In particular, the resistance assessment by mass loss through brushing was frequently criticized as a severe test condition which did not represent field conditions [44],[29]. The latter proved that using unconfined compressive strength could indicate the frost durability of soil-cement mixtures. They found good correlation between the mass loss from ASTM D560 procedures and the change in UCS. However, as it was pointed out by Narloch and Woyciechowski [26] realization of compression test on all samples is often impossible to perform if some of them experience important mass loss by scaling.

In consequence in this study, a first series of freeze-thaw tests were performed following the standard ASTM D560. This test consisted in exposing two cement-stabilized samples realized with Proctor compaction to repeat freezing-thawing. The first sample was used to calculate the water content and the volume change and the second sample allowed obtaining mass losses by scaling. During a freeze-thaw cycle, the samples were firstly exposed to a frost phase that consisted in placing them for 24 h in a freezing room set to a temperature of -23°C . Afterwards, for the thawing phase the specimens were placed in a moist room having a temperature of $+23^{\circ}\text{C}$ and a relative humidity near to 100% for 23 h. During thawing, sufficient quantity of water was put in the carrier of the specimen to allow water absorption by capillarity. As presented in **Fig. 4**, a porous disc and blotting papers as absorptive pads were placed under the specimen.

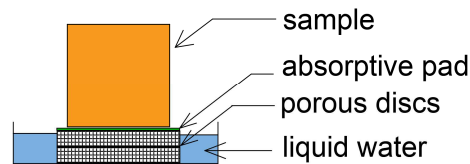


Fig. 4. Schematic of the specimen exposed to water absorption by capillary action

After each phase, the first sample was weighed with a balance of 0.1 g nearest and its measurements (diameters and heights) were recorded with an accuracy of 0.01 mm by using a caliper. For each dimensional measurement, three different points were defined on the sample. The average diameter and average height were then retained for the calculation of the sample volume. The corresponding water content and the volumetric strain were thus calculated.

As shown in **Fig. 5**, the second sample was carefully brushed on all the surfaces exposed to freezing in order to remove the scaled particles, as requested in standard ASTM D560. Then the mass loss by scaling corresponded to the difference between the weight of the second sample before and after being brushed. The cycles were repeated until either the collapse of the specimen or the reach of 12 cycles.

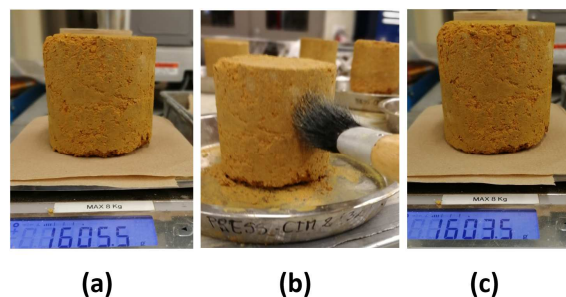


Fig. 5. Procedure for assessing mass losses by scaling: (a) first weighing before brushing the sample, (b) brushing the surface to remove the scaled particles and (c) final weighing after brushing the sample.

The moistening process by capillary absorption requested in the standard ASTM D560 is adapted to investigate the durability against the combined effect of capillary rises and freezing/thawing cycles (**Fig. 6.a**). However, it can appear too harmful in order to analyze the sole effect of freezing/thawing cycles on earthen walls at early ages, for which the saturation ratio may be sufficiently high in order to allow the freezing of the in-pore water. To analyze this scenario, an alternative protocol, without water absorption system was considered (**Fig. 6.b**). Finally, in addition to the dynamic compaction method that is prescribed in the standard, a static compaction method was used to realize the sample.

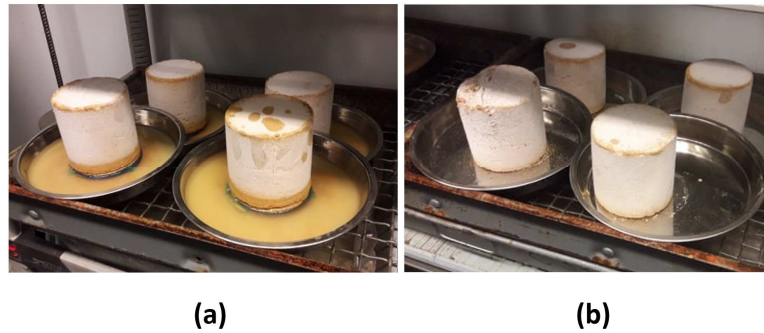


Fig. 6. Tested samples (a) with and (b) without water absorption by capillarity.

Finally, reference samples (not submitted to the freezing stage) were considered for each test conditions (that are, with/without capillary absorption) and each sample types (that are static or dynamic compaction). During all the tests, these reference samples always remained in the moist room. When a frozen sample was placed in the freezing room, its corresponding reference sample was sealed and stored. When the frozen sample was placed in the moist room for thawing period, the reference sample was then unwrapped and exposed to the same moistening process. All the measurements on reference samples were made after this moistening process. The aim of these reference samples was to distinguish the part of the damage caused by the moistening process to the one induced by the freezing-thawing one.

To conclude, four protocols on four types of samples were realized. These 16 test configurations are summarized in the **Table 3**. The mention “FT” refers to samples subjected to freeze-thaw cycles while “ref” refers to reference samples that are not submitted to freeze-thaw cycles. On the other side, “MR” and “WA” respectively denote samples without and with water absorption by capillarity. For example, the designation “PRESS-CEM-WA-FT” refers to a sample of stabilized soil compacted with the press and submitted to freezing-thawing cycles with water absorption by capillarity.

Table 3. Molding and experimental conditions of tested samples

Designation	Material	Method of compaction	Method of moistening	Freezing-thawing
PRESS-US-MR-ref	Soil	Static compaction	Moist room	No
PRESS-US-MR-FT	Soil	Static compaction	Moist room	Yes
PRESS-US-WA-ref	Soil	Static compaction	Moist room + water absorption	No
PRESS-US-WA-FT	Soil	Static compaction	Moist room + water absorption	Yes
PROC-US-MR-ref	Soil	Dynamic compaction	Moist room	No
PROC-US-MR-FT	Soil	Dynamic compaction	Moist room	Yes
PROC-US-WA-ref	Soil	Dynamic compaction	Moist room + water absorption	No
PROC-US-WA-FT	Soil	Dynamic compaction	Moist room + water absorption	Yes
PRESS-CEM-MR-ref	Soil + cement	Static compaction	Moist room	No
PRESS-CEM-MR-FT	Soil + cement	Static compaction	Moist room	Yes
PRESS-CEM-WA-ref	Soil + cement	Static compaction	Moist room + water absorption	No
PRESS-CEM-WA-FT	Soil + cement	Static compaction	Moist room + water absorption	Yes
PROC-CEM-MR-ref	Soil + cement	Dynamic compaction	Moist room	No
PROC-CEM-MR-FT	Soil + cement	Dynamic compaction	Moist room	Yes

PROC-CEM-WA-ref	Soil + cement	Dynamic compaction	Moist room + water absorption	No
PROC-CEM-WA-FT	Soil + cement	Dynamic compaction	Moist room + water absorption	Yes

3. Results

3.1. Visual inspection of freeze-thaw effects

As mentioned in Introduction, frost damage can manifest through internal cracking and surface scaling. This latter is visible when repeated freeze-thaw cycles induce a significant amount of matter peeling away from the surface. The degree of surface scaling could be considered as a good parameter to evaluate the frost susceptibility of the building material thus its frost durability. Then, visual inspection of samples can qualitatively report frost damage. The picture of all tested samples at the end of the 12 cycles are reported in **Fig. 8**. Whatever their type (i.e. PRESS-US, PRESS-CEM, PROC-US and PROC-CEM), no significant damage was observed on the reference samples over the cycles. On the opposite, damage was detected on samples submitted to freeze-thaw cycles. Therefore, it can be assumed that observed damages were mainly due to the repeated freezing-thawing cycles. In the case of unstabilized samples, frost damage followed by a total collapse of the samples was observed after only a few cycles. To illustrate that point, the evolution of the frost damage of the sample PROC-US-MR-FT between the 1st and 4th cycle is presented in **Fig. 7**. This damage firstly occurred by horizontal cracking at the interface of compaction between layers. With increasing freeze-thaw cycles, cracking also developed vertically with important swelling and scaling. In the case of stabilized specimens, no collapse was observed before 12 cycles, except for the PRESS-CEM-MR-FT and PROC-CEM-MR-FT. Nonetheless, a significant surface degradation was observed for samples exposed to freezing-thawing and when F-T cycles are associated with water absorption by capillarity, high erosion and mass losses were generated at the bottom of the frozen samples (PRESS-CEM-WA-FT and PROC-CEM-WA-FT). Such heavy scaling deterioration was also observed in assessment of frost resistance of cement-treated soils and compressed earth blocks by using the same testing protocol [47],[45]. The latter authors mentioned no damage for CEB without water absorption, whereas in this study we observed surface scaling for stabilized samples without capillary action. Even if this point should be analyzed deeper, one possible reason of this difference may be the presence of the interfaces between layers, where the scaling process seems to be initiated.

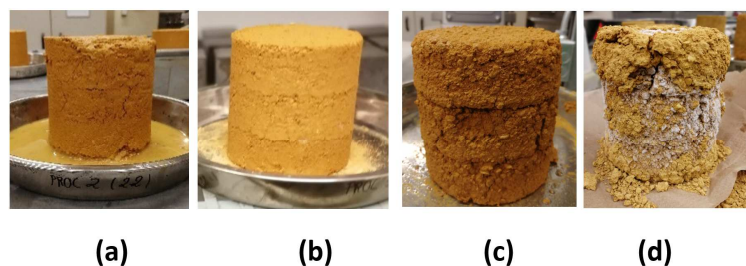


Fig. 7. Evolution of damage on the unstabilized sample PROC-US-MR-FT after (a) 1 cycle, (b) 2 cycles, (c) 3 cycles and (d) 4 cycles

	MR-ref	MR-FT	WA-ref	WA-FT
PRESS-US		 2 cycles		 2 cycles
PRESS-CEM		 5 cycles		
PROC-US		 5 cycles		 3 cycles
PROC-CEM		 11 cycles		

Fig. 8. Photos of the samples after the 12 cycles (of freezing/thawing for the FT series, or of moistening for the ref series) or when they collapse. In that case, the cycle at which the sample has collapsed is indicated below the photo.

Collapses of frozen samples (either the stabilized or the unstabilized ones) always took place after a thawing period. Two frost damage mechanisms were observed. On the one hand, for compacted unstabilized samples with water absorption (PRESS-US-WA-FT and PROC-US-WA-FT), the damage was visible with a large vertical crack; for PRESS-US-MR-FT, the crack was horizontal exactly at the interface of the 2 layers. This kind of damage appeared quickly during the experiments (before 3 cycles). On the other hand, for stabilized samples and for PROC-US-MR-FT, no major cracks were observed, but the frost damage was associated to an important scaling and also an erosion at the bottom of samples exposed to water absorption (PRESS-CEM-WA-FT and PROC-CEM-WA-FT). The scaling started to occur with repeated freezing-thawing cycles.

3.2. Wet mass variation

As aforementioned, samples were weighed after each cycle. The results are presented in **Fig. 9**. In the case of unstabilized reference samples (without frost attack), a significant increase in wet mass (between 9%

and 12% of increase) was observed and water absorption by capillarity allowed a quicker increase in wet mass during the first cycles. The unfrozen stabilized samples also increase but in a more limited extent (around 2% of mass increase).

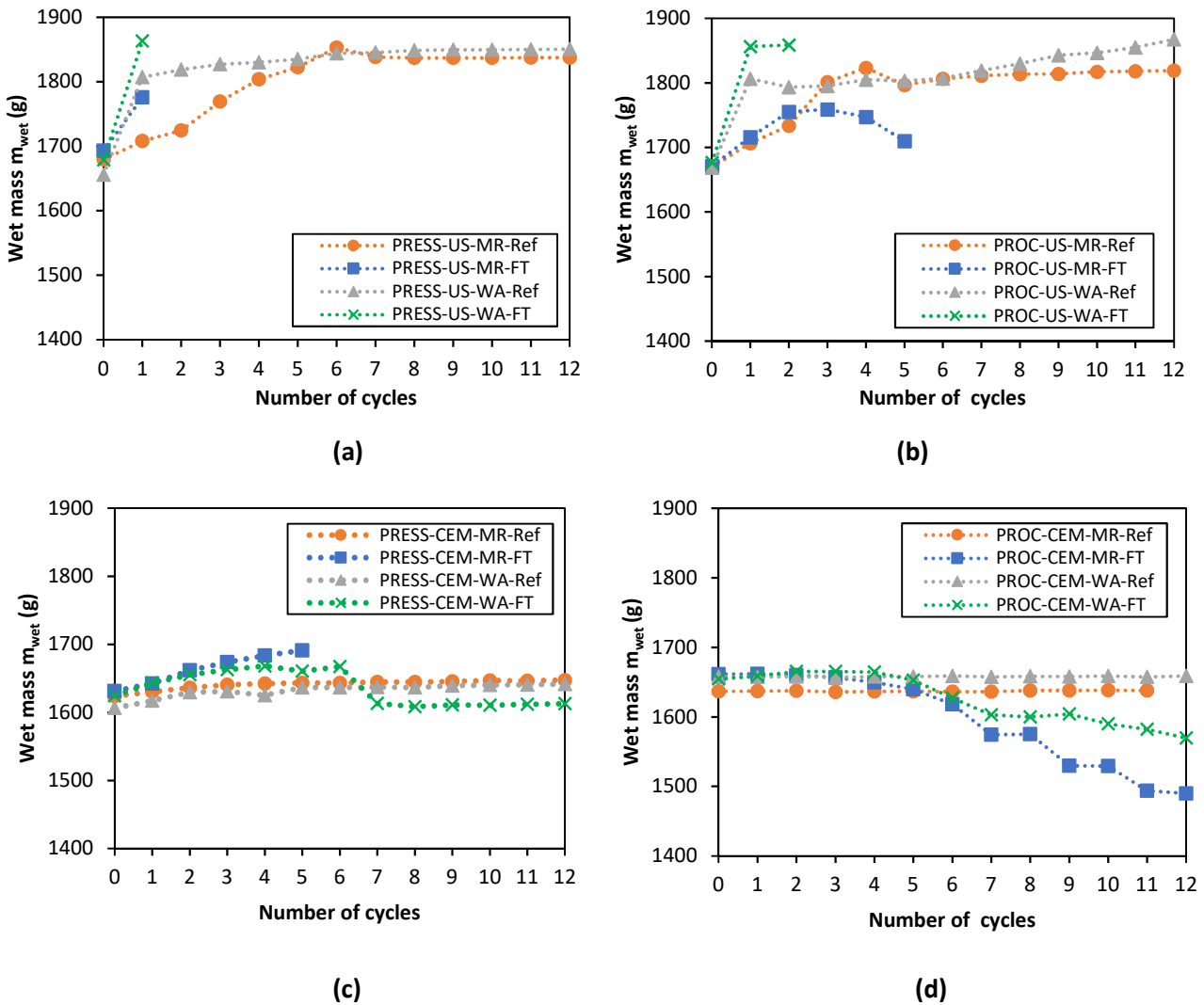


Fig. 9. Change in wet mass on PRESS (a), PROC (b), PRESS-CEM (c) and PROC-CEM (d) samples with number of cycles

For samples submitted to freezing-thawing cycles, two steps in their change in wet mass were observed. The weights increased during the first cycles (1 to between 4 and 5) afterward it started to decrease. This loss in weight was highly intense for stabilized samples, especially for those compacted by Proctor. Nonetheless, no decrease of mass was observed for PRESS-US samples and PRESS-CEM-WA-FT sample because they collapsed before the occurrence of this second stage. For stabilized samples, the results did not allow identifying clearly the difference in behavior caused by the compaction and moistening methods.

On the sole base of these first results, no accurate assessment can be made about moistening effect and surface scaling under freeze-thaw cycles. Indeed, the total mass variation measured at each cycle is a combination mass increase due to water absorption and mass decrease due to the scaling effect. Therefore, it is possible that these two phenomena (moistening and scaling) offset each other such as for PRESS-CEM-WA-FT which showed a constant wet mass after 7 cycles. Then in order to assess the frost resistance of the material, it should be better to distinguish the liquid saturation mechanism and the surface scaling. For that, under some assumptions, the evolution of wet mass will be split into two variables: the dry mass for

evaluating the mass losses by scaling and the water content for the liquid saturation effect on the durability to frost attack.

3.3. Assessment of mass loss by scaling

As aforementioned, the amount of mass loss by scaling m_{sca} was evaluated by brushing samples after each F-T cycle. Then it was possible to calculate π which represented the amount of scaled mass by a unit of area of the surface S exposed to freezing as:

$$\pi = \frac{m_{sca}}{S} \quad (2)$$

It is important to underline here that in eq (2), it is the initial surface and not the current surface which is considered. Indeed, it would be quite complicated to assess precisely this latter given the general shape of the spalled materials (cf. **Fig. 8**). This simplification should, however, be kept in mind to analyze properly the evolution of π between two cycles for deeply scaled samples.

Fig. 10.a shows a clear and strong increase of scaled mass with the number of repeated freeze-thaw cycles on unstabilized samples. For stabilized samples in **Fig. 10.b**, the amount of scaled mass was greater after 6 cycles with a peak at 7 cycles and an important decrease later. At the 7th cycle, this peak in mass loss occurred because the freezing temperature was unexpectedly limited to -2°C for more than 48 h. This observation questions the influence of freezing temperature and freezing duration on scaling. A specific experimental study should be conducted later in order to better clarify the main parameters affecting frost scaling of earthen samples. However, without considering this peak, the mass loss was limited to 0.7 kg/m^2 . As the mass loss fluctuated greatly, no clear tendency was observed; therefore it was difficult to establish any relationship with the method of compaction or the effect of water absorption by capillarity. However, these results pointed out that the mechanism of frost scaling had a severe impact on both unstabilized and stabilized samples as the number of cycles increases.

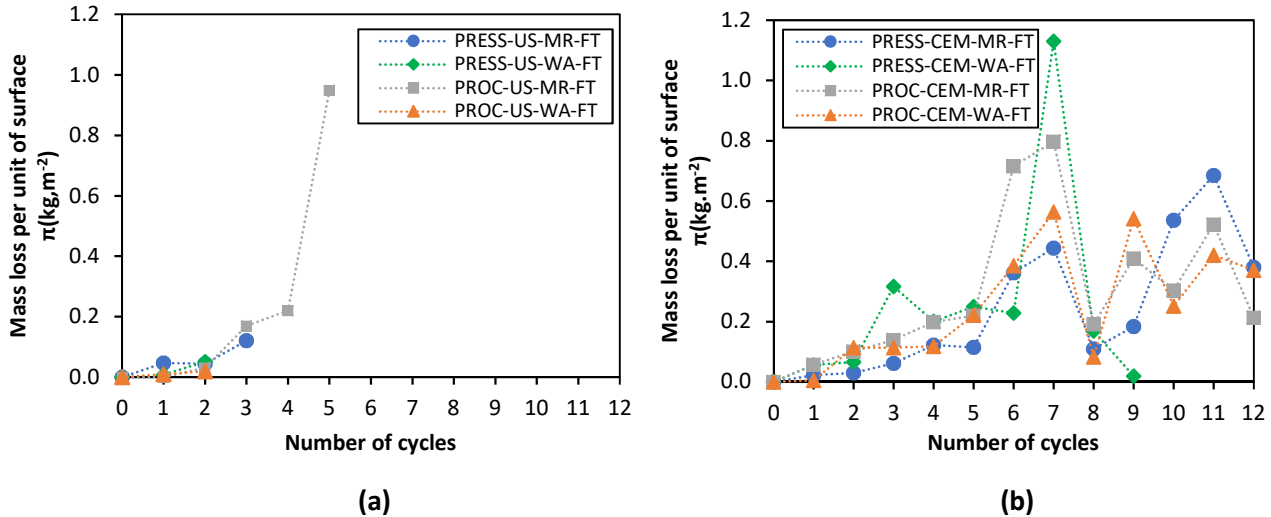


Fig. 10. Mass losses per unit of exposed surfaces of (a) unstabilized frozen samples and (b) stabilized frozen samples

4. Discussion

4.1. Calculation of dry mass change

The gross results obtained following the protocol ASTM D560 standard allow underlining clearly the strong difference in frost resistance between stabilized and unstabilized samples. However, as the wet mass merged the effect of both water absorption and surface scaling, an analysis relying on dry mass change

should be more relevant to estimate the importance of soil-cement losses thus the damage due to surface scaling.

To calculate the values of the dry mass m_d , we need to consider the effect of mass loss due to scaling given that this quantity was not negligible for a frozen sample. So, based on visual assessment of the discrepancy between frozen and unfrozen samples seen in **Fig. 8**, we can assume that scaling which is only due to freezing is the single mechanism of all the dry mass losses (then we neglect the part of mass loss due to only water erosion at the bottom of samples). Under this assumption, at any number of cycles N , the dry mass of unfrozen samples remained constant. In the case of a frozen sample, after N cycles, the dry mass m_d^N can be estimated as:

$$m_d^N = m_d^{N-1} - \frac{m_{sca}^N}{1+\omega_{sca}} \quad (3)$$

Where m_d^N and m_d^{N-1} represented the dry mass respectively at N and $N-1$ cycles, m_{sca}^N was the measured scaled mass and ω_{sca} its water content at N cycles. This water content was determined after drying the collected scaled mass and it was equal to near 6%.

The variation of dry mass of frozen samples with the number of cycles, calculated through the relation (3), is reported in **Fig. 11**. On the basis of these new results, and applying the criterion of mass loss authorized by the Portland Cement Association [40] which is 10% on the initial dry mass, it is possible to conclude that PRESS-CEM-WA-FT and PROC-CEM-WA-FT did not respect this recommendation and PROC-CEM-MR-FT was not far from the limit. All these remarks for cement-stabilized samples under freezing and thawing are more consistent with the visual inspections.

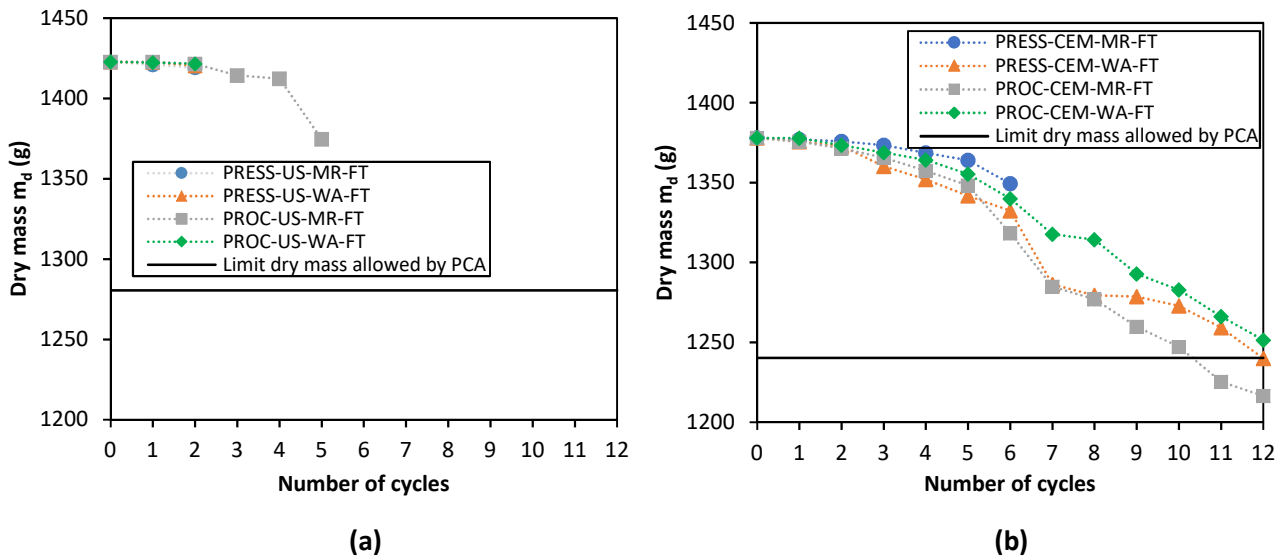


Fig. 11. Evolution of dry mass of unstabilized samples (a) and stabilized samples (b) exposed to freezing-thawing cycles

In addition, without going to early conclusion, the decrease in dry mass of Proctor compacted samples were more important, which should suggest a more important surface scaling, but the press compacted samples were more subjected to collapse (either for unstabilized and stabilized samples). As the frost cracking started from the interfaces between compacted layers of a sample (see the example of PROC-US-MR-Ft in **Fig. 7**), PROC-compact samples can be more sensitive to surface scaling because they have one more interface than PRESS-compact samples. Indeed, interface between two layers of compaction appeared to be an outset zone for freezing, and thus a weakened point to frost resistance. To analyze further these results, it would be, however, necessary to understand better the dynamic of the moistening process during the freeze-thaw cycles.

4.2. Assessment of water content change

In order to study the impact of the freezing-thawing cycles on the moistening of earthen samples, one calculated variable required by the standard ASTM D560 is the water content ω^N . It was determined for any sample after a number of N freeze-thaw cycles as follows:

$$\omega^N = \left(\frac{m_w^N}{m_d^N} - 1 \right) \quad (4)$$

where m_w^N and m_d^N are respectively the wet mass (see Fig. 9) and the dry mass (see Fig. 11) of a specimen after N cycles.

As shown in Fig. 12, it is observed that for any compaction method (Press or Proctor; static or dynamic) and any soil mixture (with or without cement), the maximum water contents reached by frozen samples are clearly higher than the values reached by the unfrozen samples. In addition, the comparisons Fig. 12.a vs Fig. 12.b and Fig. 12.c vs Fig. 12.d show significant differences in function of the compaction process and the type of soil mixtures.

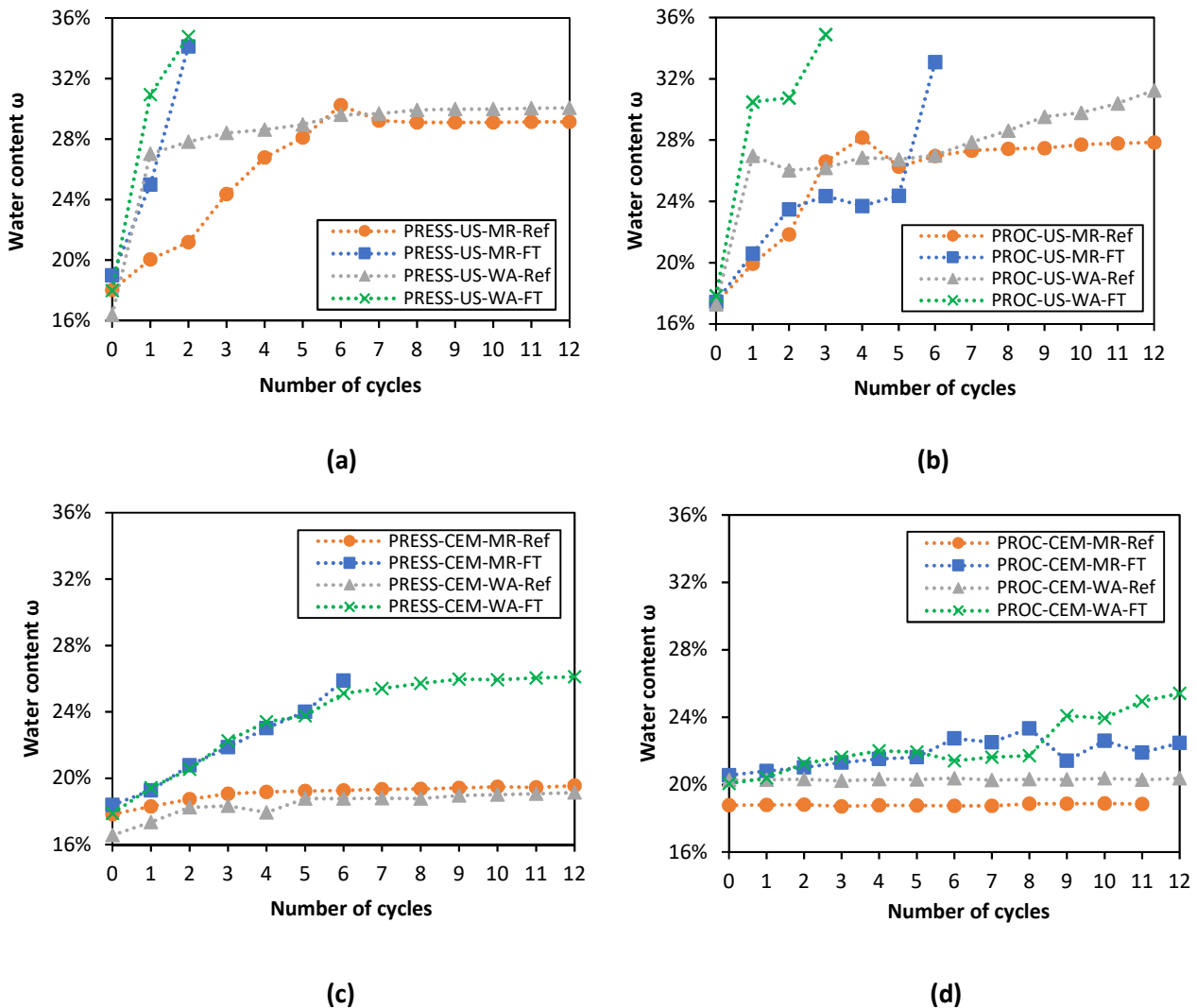


Fig. 12. Changes in water content with the number of cycles on PRESS-US (a), PROC-US (b), PRESS-CEM (c) and PROC-CEM (d) samples

For unstabilized samples without freeze exposure, an increase in water content occurred during the first 6 cycles. This increase was faster for samples with WA. Since the 6th cycle, the values remained constant

around 27% to 30% except for PROC-US-WA-Ref which continued to absorb water until the end of the test. The unfrozen unstabilized samples became more and more wet with increasing number of cycles until they seemed fully saturated. But a huge gap was clearly observed with frozen samples whose water content reached near to 35%. For stabilized samples, the reference samples did not exhibit any significant rise in water content whereas the frozen cement-treated samples showed a more visible increase in water content. The maximum water content reached by stabilized specimens was around 25% - 26%.

The static-compacted samples presented more homogeneous tendencies than the dynamic compacted samples. In fact, the final maximal value of water content reached by the press-compacted samples is not impacted by the moistening method. Precisely, PRESS-US-MR-Ref and PRESS-US-WA-Ref (id PRESS-US-MR-FT and PRESS-US-WA-FT) had almost same points of convergence in water content and PRESS-CEM-WA-Ref and PRESS-CEM-WA-Ref (id PRESS-CEM-MR-FT and PRESS-CEM-WA-FT) presented a similar evolution in water content. But considering the moistening method for PROC-compacted samples, the results were more scattered.

However, water absorption by capillarity significantly fastened the water uptake kinetic during the first cycles in the case of unstabilized specimen. This tendency was not observed for stabilized samples. It might be induced by their lower absorption coefficient (A-value) compared with unstabilized samples (**Table 1**). However, given the limited amount of water uptake within stabilized samples, this result might not be significant.

Knowing the porosity ϕ and initial dry density of the samples, denoted by ρ_d^0 , it is possible to calculate the theoretical maximal water content that the sample can reach if no deformation occurs, denoted by ω_M^{th} , through the relation:

$$\omega_M^{th} = \frac{\rho_L}{\rho_d^0} \phi \quad (5)$$

With $\rho_L = 0.997 \text{ g.cm}^{-3}$ the mass density of liquid water

Whatever the type of sample (unstabilized or stabilized), values of ω_M^{th} around 21% are obtained, which is significantly lower than the maximal values effectively reached by the samples. This difference can be caused by the volumetric deformation of the sample, which tends to lower its dry density, and thus to increase its maximal water content.

4.3. Calculation of volume change and estimation of the liquid saturation degree

To analyze that last point, the direct measurement of height and diameter was made after each F-T cycle, which permitted to estimate the average volume of the specimen. The relative volume change after N number of F-T cycles can then be acquired by calculating the apparent volumetric strain ϵ^N as:

$$\epsilon^N = \left(\frac{V^N - V^0}{V^0} \right) \quad (6)$$

Where V^0 and V^N refer to the initial volume of the specimen and its current volume after N cycles respectively.

In order to interpret correctly the physical meaning of ϵ^N it is important to notice that it is in fact a combination of two opposite phenomena: on one side a global swelling of the material due to water ingress and frost damage and, on the other side, a global volume reduction due to scaling. In fact, a global swelling of the material combined with a large scaling may result in a negative value of ϵ^N .

The evolution of the apparent volumetric strains with the number of cycles was plotted in **Fig. 13**.

The results show an upward trend in volumetric strains with fluctuations, which can be attributed to both measurement errors given by caliper in the case of stabilized samples and weakened state of unstabilized

samples when they became saturated. Along the same line, the heterogeneity of the scaling process induced important uncertainties in diameter measurements of highly scaled samples.

Nevertheless, some general tendencies are still observable. For unstabilized soils (**Fig. 13.a** and **Fig. 13.b**), the volume change was depicted with a strong expansion near to 20%. In comparison, stabilized soils (**Fig. 13.c** and **Fig. 13.d**) exhibited quite limited volume expansion, which did not exceed 5%. This reduction of swelling due to cement addition was quite expected, since this latter was classically used for the treatment of expansive soils [48]. Going into details, the Proctor compacted samples, either stabilized or unstabilized and whatever tests configurations, tend to a slightly more important swelling than the press compacted samples.

Since they collapsed quite rapidly, it is difficult to analyze the impact of freeze-thaw cycles on unstabilized samples. The only remark that can be done for these samples is the stronger swelling in the first cycles, when capillary absorption is present. For cement-stabilized samples, even if it is not obvious, the repeated freeze-thaw cycles induce a slight increase of volume change.

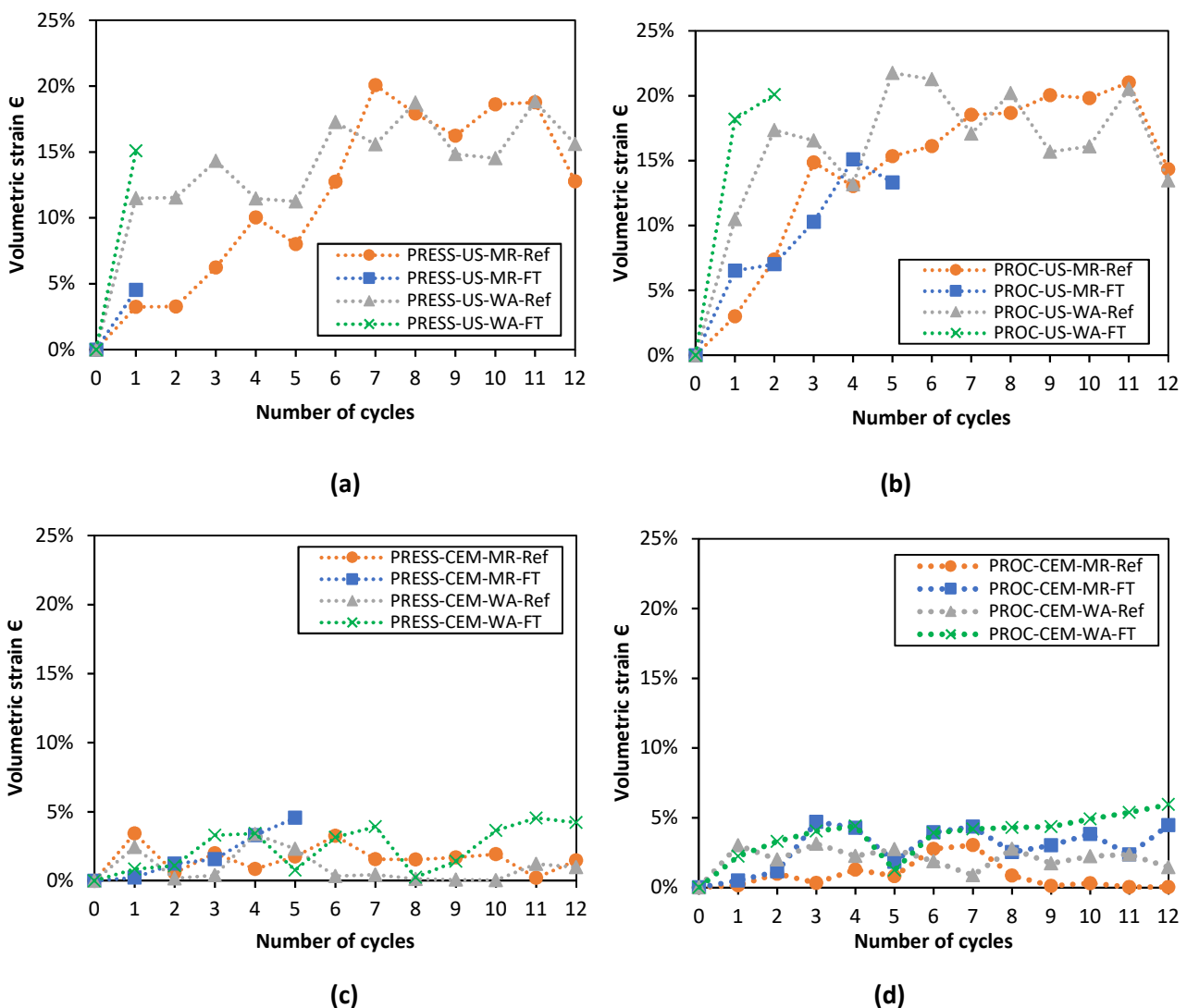


Fig. 13. Volumetric strain of PRESS (a), PROC (b), PRESS-CEM (c) and PRO-CEM samples (d) with a number of cycles

In order to go further on the analysis of the water content data and the volume variations of the samples, it is now possible to have an estimation of the sample's degree of saturation that is the ratio between the

water volume and the pore volume, and of its evolution with freeze-thaw cycles. At any cycle N, this latter, denoted by S_L^N , can be calculated through the following relation:

$$S_L^N = \frac{\omega^N}{\rho_L \left(\frac{1}{\rho_d^N} - \frac{1}{\rho_S} \right)} \quad (7)$$

Where ω^N is the water content at N cycles, ρ_L is the liquid density, ρ_S is the skeleton density and ρ_d^N is the dry density at N cycles which is equal to:

$$\rho_d^N = \frac{m_d^N}{V^0(1+\epsilon^N)} \quad (8)$$

The variation of the degree of saturation with the number of cycles was plotted in **Fig. 14**.

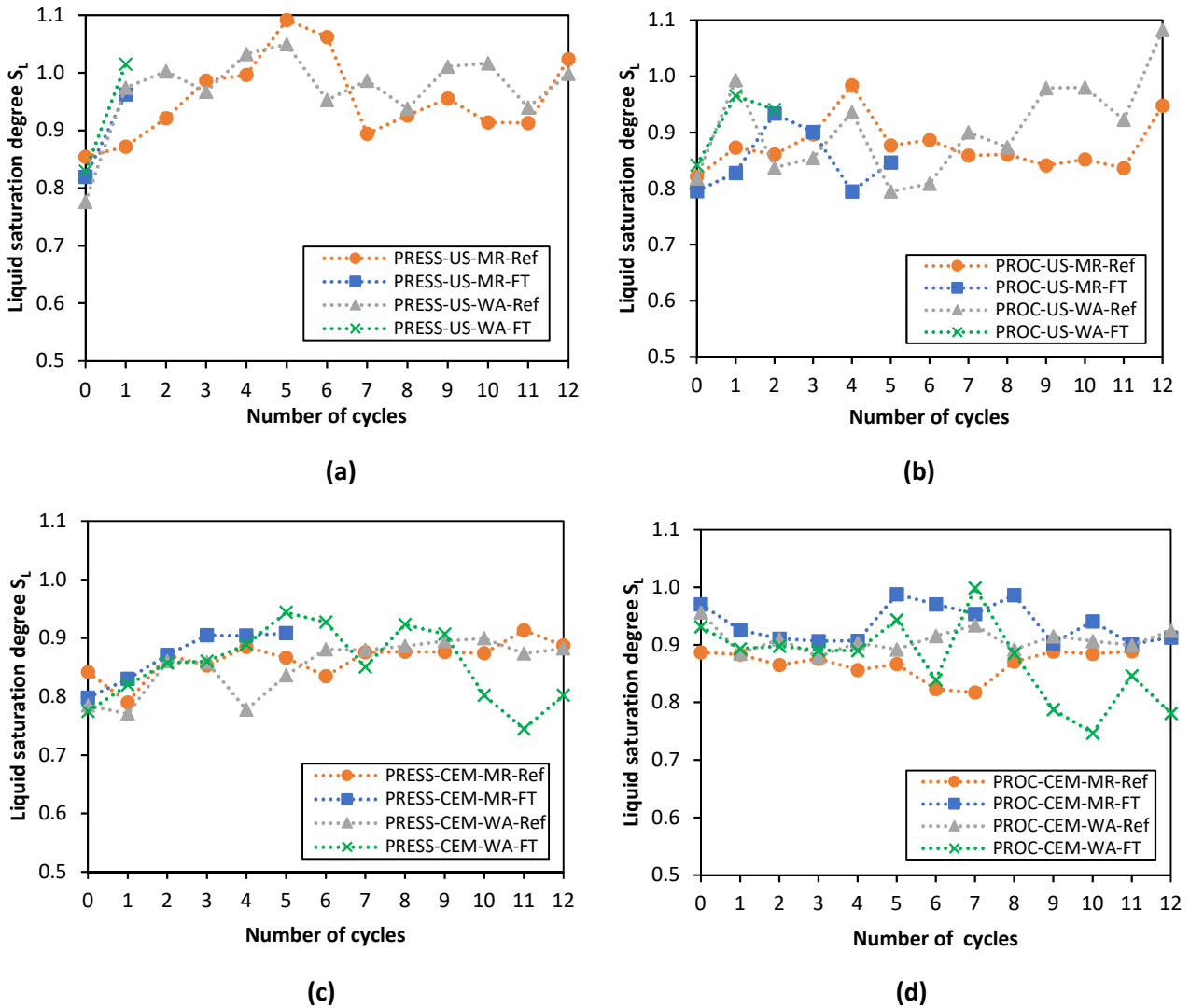


Fig. 14. Change in liquid saturation with a number of cycles of PRESS (a), PROC (b), PRESS-CEM (c) and PROC-CEM (d) samples

For any sample, saturation was higher than 80% at the beginning. One can underline the specific case of PROC-CEM samples whose liquid saturation degrees started from 90% to almost 100%. This might be attributed to an important water absorption during the seven days of cure after molding. For these samples, the liquid saturation remains stable with repeated cycles, whereas it increased to reach values between 90% and 100% for other samples. For unfrozen samples without freezing, the liquid saturation exceeded

sometimes 100% that can be explained by errors in measurements, particularly on the volume variations. When exposed to freezing-thawing cycles, cement-treated samples presented a reduction of the saturation ratio between the 7th and the 9th freeze-thaw cycles. However, this reduction may be artificially induced by large mass loss by scaling which occurs within these cycles, which tends to increase significantly the uncertainties in the saturation ratio calculations.

Anyway, this calculation of the degree of liquid saturation allows having a better idea of the physical process that has led to the increase of water in samples submitted to freeze-thaw cycles. Indeed, this latter is not only due to an ingress of water within the pore space up to its full saturation. A clear link between the swelling of the materials and the increase of water content was underlined by the fact that the degree of saturation remains almost constantly close to 1. It follows that, the deformation of the pore space due to the formation of the ice crystal, combined with additional ingress of water either by capillary condensation or water absorption during the thawing stage had both played a main role in the increasing ingress of water within the material. In consequence, even if no collapse had occurred, a significant and irreversible deformation had happened during the freeze-thaw cycles, which may modify the mechanical behavior of the material even after its complete thawing and drying. Indeed, Narloch and Woyciechowski [26] observed that cracks developed during the freezing-thawing cycles of stabilized rammed earth led to an increase in water absorption, loss in mass and decrease in compressive strength. Same kind of results were obtained by Lu et al [18], [48] on soil-cement mixtures and by Walker and Karabulut [49] on soil-lime mixtures. Finally, Bryan [50] observed a permanent dilation after freeze/thaw cycles on cement-soil mixtures.

4.4. Consistency and limits of results and test method

From the standardized freeze-thaw test protocol ASTM D560, assessment of frost impact on earthen materials was made considering different factors as compacting method, cement-stabilization and capillary rise. This standard does not have a requirement on the soil type, except the granulometry of the soil for the test specimen. The standard requires sieving the soil at 4.75 mm and a 5 mm sieve was used, which should have a negligible impact on the results.

Visual inspection, dry mass evolution and amount of mass loss by scaling gave all consistent results in spite of the variability inherent to brushing procedures. They were found to be good indicators of frost damage, especially for unstabilized samples. Indeed, the early collapse of unstabilized samples does not allow making a proper comparison of the data obtained with these three methods. On the contrary, the analysis of the wet mass was found inaccurate because it addresses two distinct phenomena, which are the mass increase due to water uptake and the mass decrease due to scaling.

The experimental results showed that freeze-thaw cycles lead to noticeable increases in water content and swelling. It can be explained by two main physical processes. At first, when water phase change occurs in porous media, ice expansion generates in-pore deformations and cracking. Additional porous space is then created and it can be filled by water during the thawing stage. During that stage, the sample that is still partially frozen will be in contact with liquid water. In such case, the ingress of water within the material may be fastened by the cryo-suction process, which is driven by gradient in chemical potential between water at the vicinity of ice crystals and free water, far from the thawing front. This second phenomenon may explain why the water uptake is faster for samples submitted to freeze-thaw cycles than for reference samples stored in moist room or submitted to capillary absorption test. Nevertheless, water absorption coefficient (A-value) could not predict the behavior of samples when subjected to freeze-thaw cycles. No clear relationship was identified between A-value and loss in mass, water content and volume change. Bryan [50] explained that A-value just identified how samples would be saturated and then susceptible to frost attack. But no link between A-value and frost resistance is established yet. Let us finally underline that water content and swelling increases were more noteworthy in the first cycles. This observation is consistent with previous studies realized on the impact of freeze-thaw cycles on soils regarding their physical parameters, such as the void ratio, hydraulic conductivity [20], dry density [33], cohesion [14] or some mechanical properties such as unconfined compressive strength and resilient modulus [52].

The goal of this study was to estimate the frost resistance under the most prejudicial cases, which are the early age (i.e. just after fabrication and thus before the wall has had time to dry) and the pathological case of capillary water rise. However, even to test such conditions, the test protocol used in this study may be too severe. At first, it would be more representative to test lighter frost conditions, with temperature variations closer to 0°C. Indeed, the freeze-thaw cycles from -23° to +23°C in two days that are prescribed in the ASTM D560 are very harsh and do not happen in reality. The testing protocol was more representative of frozen soils and permafrost. For earthen houses, the temperature changes are usually milder. Unless in the very Nordic latitude, -23°C does not last for very long, especially not in the ground, and it is commonly not followed by such rapid thawing conditions. As samples are moved from freezing chamber to moist chamber, ASTM D560 considered instantaneous variations of temperature that are far from the kinetics of freezing/thawing underwent in reality by earthen houses. This process should be investigated further in the evaluation of frost damage. Anyway, even if the air might exceptionally reach -23 °C, the core of the earthen wall will not reach this temperature. An experimental analysis of the representativeness of laboratory tests and real durability of frozen earthen materials were addressed by Seco et al. [53]. Their samples were less damaged under real outdoor conditions than under laboratory F-T cycles. The authors highlighted that laboratory F-T tests were not good estimator for real frost resistance of earth-based constructions.

Secondly, it would be interesting to consider thawing stages under lower relative humidity conditions. Indeed, the use of the moist room was found to induce water content levels nearly as high as those of capillary absorption conditions, which can reasonably appear to be too severe.

Finally, all the tests were made on small samples, for which the temperature remained almost homogenous during the whole test (except during the transitional periods of the freezing and thawing stages). However, in reality, strong thermal gradients are expected in earthen walls, especially under winter condition. This aspect should be treated in the near future in order to properly identify all the phenomena involved in the frost damage of earthen walls.

5. Conclusions

The main purpose of this paper is to assess the frost resistance of earthen buildings exposed to cycles of freezing-thawing. Two kinds of tests were performed following procedures similar to the ASTM D-560 (twelve cycles of -23°C/ +23°C). In the former, samples were submitted to capillary absorption during the thawing stage, in order to evaluate the combined effect of capillary rise and frost action. In the second one, samples were tested at their initial water content at manufacture and the thawing stage occurred in a moist room. The goal of this test condition was to estimate the frost resistance at early age, before the drying of the earthen wall protects it from the deleterious effect of freeze-thaw cycles. Whatever the test condition, frost damage was evaluated through the change in volume, the mass loss by scaling and the water uptake at different F-T cycles. The results obtained lead to the main conclusions as follows.

Under freezing-thawing cycles, both unstabilized and stabilized samples experienced significant scaling, increase in volume and water content. Nonetheless, impact of F-T cycles on stabilized samples was largely decreased compared to unstabilized samples. These latter all collapsed during the first six freeze-thaw cycles. These results confirm the poor resistance against frost attacks of unstabilized compacted earth at early ages and/or submitted to a pathologic ingress of water. However, this does not mean that earth is not able to withstand freeze-thaw in its normal state of use i.e. with low saturation ratios, as proved by many time-tested buildings in real conditions.

Swelling and scaling caused by freeze-thaw cycles for both stabilized and unstabilized samples were more significant for dynamic Proctor-compacted samples than static press-compacted samples. On the other side, press compaction allowed more regular and higher water absorption than Proctor compaction, particularly for stabilized samples. Moreover, the total collapse was found to be more likely to happen on press compacted samples. However, additional studies are needed to draw a final conclusion on the impact of compaction methods regarding the frost resistance of earthen buildings.

Even if capillary absorption may induce a slight increase in frost damage, the general tendency observed for the two test conditions were similar. It can be explained by the very close water content levels reached by the sample, whatever the protocol used for the thawing stage. This result led to the conclusion that the use of the moist room to analyze the early age resistance may be too severe, and thus, that more moderate conditions should be tested in the future. In the same spirit, amplitude and kinetics of the cycles should be improved to be more representative of real environmental conditions. But for these purposes, additional information is needed on the real atmospheric conditions (RH, T) to which earthen walls are submitted in function of their geographical location. Finally, it would be interesting to setup adapted protocols to test the frost resistance in less prejudicial conditions than the early age and the pathological case of capillary rises.

Acknowledgements

The authors acknowledge Stephane Cointet and Alexis Vadeboncoeur for their technical support, as well as Victor Brial and Meriem Aouinti who contributed to the experimental tests.

References

- [1] J.-C. Morel, M.A. Mesbah, M. Oggero, P. Walker, Building houses with local materials: Means to drastically reduce the environmental impact of construction, *Build. Environ.* (2001) 1119–1126. [https://doi.org/10.1016/S0360-1323\(00\)00054-8](https://doi.org/10.1016/S0360-1323(00)00054-8).
- [2] A. Fabbri, J.-C. Morel, Earthen materials and constructions, *Nonconv. Vernac. Constr. Mater.* 10. (2016) 273–299.
- [3] F. McGregor, A. Heath, A. Shea, M. Lawrence, The moisture buffering capacity of unfired clay masonry, *Build. Environ.* 82 (2014) 599–607. <https://doi.org/10.1016/j.buildenv.2014.09.027>.
- [4] F. Champiré, A. Fabbri, J.-C. Morel, H. Wong, F. McGregor, Impact of relative humidity on the mechanical behavior of compacted earth as a building material, *Constr. Build. Mater.* 110. (2016) 70–78.
- [5] Q.-B. Bui, J.-C. Morel, S. Hans, P. Walker, Effect of moisture content on the mechanical characteristics of rammed earth, *Constr. Build. Mater.* 54. (2014) 163–169.
- [6] P. Scarato, J. Jeannet, *Cahier d'expert bâti en pisé- Connaissance, analyse, traitement des pathologies du bâti en pisé en Rhône-Alpes et Auvergne*, ABITerre, Rhône-Alpes, 2015.
- [7] S. J. Marchand E. J. and M. Pigeon, Deicer Salt Scaling Deterioration--An Overview, *ACI Symp. Publ.* 145 (1994). <https://doi.org/10.14359/4539>.
- [8] J.J. Valenza, G.W. Scherer, Mechanisms of salt scaling, *Mater. Struct.* 38 (2005) 479–488. <https://doi.org/10.1007/BF02482144>.
- [9] A. Fabbri, O. Coussy, T. Fen-Chong, P. Monteiro, Are Deicing Salts Necessary to Promote Scaling in Concrete ?, *J. Eng. Mech. ASCE* 1347. (2007) 589–598.
- [10] T.C. Powers, *The air requirement of frost-resistant concrete*, [Portland Cement Association], [Chicago], 1949.
- [11] T.C. Powers, R.A. Helmuth, *Theory of volume changes in hardened Portland cement paste during freezing*, [Portland Cement Association], Chicago, 1953.
- [12] M.J. Setzer, Micro-Ice-Lens Formation in Porous Solid, *J. Colloid Interface Sci.* 243 (2001) 193–201. <https://doi.org/10.1006/jcis.2001.7828>.
- [13] J.-M. Konrad, Physical processes during freeze-thaw cycles in clayey silts, *Cold Reg. Sci. Technol.* 16 (1989) 291–3063. [https://doi.org/10.1016/0165-232X\(89\)90029-3](https://doi.org/10.1016/0165-232X(89)90029-3).
- [14] A. Hotineanu, M. Bouasker, A. Aldaood, M. Al-Mukhtar, Effect of freeze–thaw cycling on the mechanical properties of lime-stabilized expansive clays, *Cold Reg. Sci. Technol.* (2015) 7.
- [15] G.W. Scherer, Freezing gels, *J. Non-Cryst. Solids.* 155 (1993) 1–25. [https://doi.org/10.1016/0022-3093\(93\)90467-C](https://doi.org/10.1016/0022-3093(93)90467-C).
- [16] G.W. Scherer, Crystallization in pores, *Cem. Concr. Res.* 29 (1999) 1347–1358. [https://doi.org/10.1016/S0008-8846\(99\)00002-2](https://doi.org/10.1016/S0008-8846(99)00002-2).
- [17] O. Coussy, Poromechanics of freezing materials, *J. Mech. Phys. Solids* 53. (2005) 1689–1718.

- [18] Y. Lu, S. Liu, E. Alonso, L. Wang, L. Xu, Z. Li, Volume changes and mechanical degradation of a compacted expansive soil under freeze-thaw cycles, *Cold Reg. Sci. Technol.* 157 (2019) 206–214. <https://doi.org/10.1016/j.coldregions.2018.10.008>.
- [19] S. Xie, J. Qu, Y. Lai, Z. Zhou, X. Xu, Effects of freeze-thaw cycles on soil mechanical and physical properties in the Qinghai-Tibet Plateau, *J. Mountain Sci.* 12 (2015) 999–1009.
- [20] J.-M. Konrad, Effect of freeze–thaw cycles on the freezing characteristics of a clayey silt at various overconsolidation ratios, *Can. Geotech. J.* 26 (1989) 217–226. <https://doi.org/10.1139/t89-031>.
- [21] M. Rosenqvist, K. Fridh, M. Hassanzadeh, Macroscopic ice lens growth in hardened concrete, *Cem. Concr. Res.* 88 (2016) 114–125. <https://doi.org/10.1016/j.cemconres.2016.06.008>.
- [22] S. Taber, The Mechanics of Frost Heaving, *J. Geol.* 38 (1930) 303–317. <https://doi.org/10.1086/623720>.
- [23] G. Fagerlund, The international cooperative test of the critical degree of saturation method of assessing the freeze/thaw resistance of concrete, *Matér. Constr.* 10 (1977) 231–253. <https://doi.org/10.1007/BF02478694>.
- [24] J.E. Aubert, M. Gasc-Barbier, Hardening of clayey soil blocks during freezing and thawing cycles, *Appl. Clay Sci.* 65–66 (2012) 1–5. <https://doi.org/10.1016/j.clay.2012.04.014>.
- [25] C.T.S. Beckett, P.A. Jaquin, J.-C. Morel, Weathering the storm: A framework to assess the resistance of earthen structures to water damage, *Constr. Build. Mater.* 242 (2020) 118098. <https://doi.org/10.1016/j.conbuildmat.2020.118098>.
- [26] P. Narloch, P. Woyciechowski, Assessing Cement Stabilized Rammed Earth Durability in A Humid Continental Climate, *Buildings.* 10 (2020) 26. <https://doi.org/10.3390/buildings10020026>.
- [27] I. Netinger, M. Vracevic, J. Ranogajec, S. Vucetic, Evaluation of brick resistance to freeze / thaw cycles according to indirect procedures, *Gradjevinar.* 66 (2014) 197–209. <https://doi.org/10.14256/JCE.956.2013>.
- [28] Liang Yuming, Experimental study on frost resistance of rammed earth building materials, *Chem. Eng. Trans.* 66 (2018) 1177–1182. <https://doi.org/10.3303/CET1866197>.
- [29] S.A. Shihata, Z.A. Baghdadi, Simplified Method to Assess Freeze-Thaw Durability of Soil Cement, *J. Mater. Civ. Eng.* 13 (2001) 243–247. [https://doi.org/10.1061/\(ASCE\)0899-1561\(2001\)13:4\(243\)](https://doi.org/10.1061/(ASCE)0899-1561(2001)13:4(243)).
- [30] H.B. Seed, Stability and Swell Pressure Characteristics of Compacted Clays, *Clays Clay Miner.* 3 (1954) 483–504. <https://doi.org/10.1346/CCMN.1954.0030140>.
- [31] E. Ekwue, Effect of dynamic and static methods of compaction on soil strength, *West Indian J. Eng.* 37 (2015) 74–78.
- [32] M. Olivier, Le matériau terre, compactage, comportement, application aux structures en bloc sur terre, 1994.
- [33] H. Van Damme, H. Houben, Earth concrete. Stabilization revisited, *Cem. Concr. Res.* 114 (2018) 90–102. <https://doi.org/10.1016/j.cemconres.2017.02.035>.
- [34] K.K.G.K.D. Kariyawasam, C. Jayasinghe, Cement stabilized rammed earth as sustainable construction material, *Constr. Build. Mater.* (2016) 519–527.
- [35] C. Ouellet-Plamondon, C. Soro N., M.-J. Nollet, Characterization, Mix Design, Mechanical Testing of Earth Materials, Stabilized and Unstabilized, for Building Construction, *Poromechanics VI ASCE.* (2017).
- [36] F. McGregor, A. Heath, E. Fodde, A. Shea, Conditions affecting the moisture buffering measurement performed on compressed earth blocks, *Build. Environ.* 75 (2014) 11–18. <https://doi.org/10.1016/j.buildenv.2014.01.009>.
- [37] A. Arrigoni, A.-C. Grillet, R. Pelosato, G. Dotelli, C.T.-S. Becket, M. Woloszyn, D. Ciancio, Reduction of rammed earth’s hygroscopic performance under stabilisation: an experimental investigation, *Build. Environ.* 115. (2017) 358–367.
- [38] ASTM International, ASTM D560 / D560M-16, Standard Test Methods for Freezing and Thawing Compacted Soil-Cement Mixtures, 2016.
- [39] P.-A. Chabriac, Mesure du comportement hygrothermique du pisé, *Matériaux, Ecole Nationale des Travaux Publics de l’Etat*, 2014.
- [40] Portland Cement Association, Soil-cement laboratory handbook, 1992.

- [41] ASTM International, ASTM D558 / D558M-19, Standard Test Methods for Moisture-Density (Unit Weight) Relations of Soil-Cement Mixtures, 2019.
- [42] A. Fabbri, L. Soudani, F. McGregor, J.-C. Morel, Analysis of the water absorption test to assess the intrinsic permeability of earthen materials, *Constr. Build. Mater.* 199 (2019) 154–162. <https://doi.org/10.1016/j.conbuildmat.2018.12.014>.
- [43] K. Sujata, H.M. Jennings, Formation of a Protective Layer During the Hydration of Cement, *J. Am. Ceram. Soc.* 75 (1992) 1669–1673. <https://doi.org/10.1111/j.1151-2916.1992.tb04243.x>.
- [44] K.P. George, D.T. Davidson, Development of a Freeze-Thaw Test for Design of Soil-Cement, (n.d.) 20.
- [45] K. Mak, C. MacDougall, A. Fam, Freeze-Thaw Performance of On-Site Manufactured Compressed Earth Blocks: Effect of Water Repellent and Other Additives, *J. Mater. Civ. Eng.* 28 (2016) 04016034. [https://doi.org/10.1061/\(ASCE\)MT.1943-5533.0001512](https://doi.org/10.1061/(ASCE)MT.1943-5533.0001512).
- [46] G. Strypsteen, Z. Sierens, M. Joseph, J. Benoot, L. Boehme, Freeze-thaw resistance of stabilized soils in Flanders, *Int. J. Environ. Stud.* 74 (2017) 603–612. <https://doi.org/10.1080/00207233.2017.1335021>.
- [47] D.C. Merrill, J.M. Hoover, Laboratory Freeze-Thaw Tests of Portland Cement-Treated Granular Bases, (1968) 14.
- [48] Y. Lu, S. Liu, Y. Zhang, Z. Li, L. Xu, Freeze-thaw performance of a cement-treated expansive soil, *Cold Reg. Sci. Technol.* 170 (2020) 102926. <https://doi.org/10.1016/j.coldregions.2019.102926>.
- [49] R.D. Walker, C. Karabulut, Effect of Freezing and Thawing on Unconfined Compressive Strength of Lime-Stabilized Soils, (n.d.) 11.
- [50] A.J. Bryan, Criteria for the suitability of soil for cement stabilization, *Build. Environ.* 23 (1988) 309–319. [https://doi.org/10.1016/0360-1323\(88\)90037-6](https://doi.org/10.1016/0360-1323(88)90037-6).
- [51] J. Qi, W. Ma, C. Song, Influence of freeze–thaw on engineering properties of a silty soil, *Cold Reg. Sci. Technol.* 53 (2008) 397–404. <https://doi.org/10.1016/j.coldregions.2007.05.010>.
- [52] J. Lu, M. Zhang, X. Zhang, W. Pei, J. Bi, Experimental study on the freezing–thawing deformation of a silty clay, *Cold Reg. Sci. Technol.* 151 (2018) 19–27. <https://doi.org/10.1016/j.coldregions.2018.01.007>.
- [53] A. Seco, P. Urmeneta, E. Prieto, S. Marcelino, B. García, L. Miqueleiz, Estimated and real durability of unfired clay bricks: Determining factors and representativeness of the laboratory tests, *Constr. Build. Mater.* 131 (2017) 600–605. <https://doi.org/10.1016/j.conbuildmat.2016.11.107>.